SCIENTIFIC REPORTS

Nuclear factor-κB plays a critical role in both intrinsic and acquired resistance against endocrine therapy in human breast cancer cells

Kumiko Oida[1,2], Akira Matsuda[3], Kyungsook Jung[4], Yan Xia[1], Hyosun Jang[1], Yosuke Amagai[1], Ginnae Ahn[4], Sho Nishikawa[1], Saori Ishizaka[1], Erika Jensen-Jarolim[2,5], Hiroshi Matsuda[1,3] & Akane Tanaka[1,4]

[1]Cooperative Major in Advanced Health Science, Graduate School of Bio-Applications and System Engineering, Tokyo University of Agriculture and Technology, 3-5-8 Saiwai-cho, Fuchu, Tokyo 183-8509, Japan, [2]Comparative Medicine, Messerli Research Institute of the University of Veterinary Medicine Vienna, Medical University of Vienna, University of Vienna, Veterinaerplatz 1, 1210 Vienna, Austria, [3]Laboratory of Veterinary Molecular Pathology and Therapeutics, Division of Animal Life Science, Institute of Agriculture, Tokyo University of Agriculture and Technology, 3-5-8 Saiwai-cho, Fuchu, Tokyo 183-8509, Japan, [4]Laboratory of Comparative Animal Medicine, Division of Animal Life Science, Institute of Agriculture, Tokyo University of Agriculture and Technology, 3-5-8 Saiwai-cho, Fuchu, Tokyo 183-8509, Japan, [5]Comparative Immunology and Oncology, Institute of Pathophysiology and Allergy Research, Center of Pathophysiology, Infectiology and Immunology, Medical University of Vienna, Waehringer Guertel 18-20, A-1090 Vienna, Austria.

Since more than 75% of breast cancers overexpress estrogen receptors (ER), endocrine therapy targeting ER has significantly improved the survival rate. Nonetheless, breast cancer still afflicts women worldwide and the major problem behind it is resistance to endocrine therapy. We have previously shown the involvement of nuclear factor-κB (NF-κB) in neoplastic proliferation of human breast cancer cells; however, the association with the transformation of ER-positive cells remains unclear. In the current study, we focused on roles of NF-κB in the hormone dependency of breast cancers by means of ER-positive MCF-7 cells. Blocking of NF-κB signals in ER-negative cells stopped proliferation by downregulation of D-type cyclins. In contrast, the MCF-7 cells were resistant to NF-κB inhibition. Under estrogen-free conditions, the ER levels were reduced when compared with the original MCF-7 cells and the established cell subline exhibited tamoxifen resistance. Additionally, NF-κB participated in cell growth instead of the estrogen-ER axis in the subline and consequently, interfering with the NF-κB signals induced additive anticancer effects with tamoxifen. MMP-9 production responsible for cell migration, as well as the cell expansion *in vivo*, were suppressed by NF-κB inhibition. Therefore, we suggest that NF-κB is a master switch in both ER-positive and ER-negative breast cancers.

About 75% of breast cancers overexpress the receptors for estrogen, which are dependent on the hormone for their continual development[1]. Estrogen receptors (ER) contain 2 subtypes, namely, ERα and ERβ, and are the main regulators of target gene expression. In addition, they function in conjunction with transcription factors to mediate the actions of the hormone 17β-estradiol (estrogen) in ER-positive tissues[2,3]. In general, the patients who are diagnosed as ER-positive have better outcomes compared with those who have ER-negative breast cancers. This is due to less aggressiveness of hormone-dependent cancers and the existence of endocrine therapies as a first-line treatment for the disease[4–6]. The therapeutic strategies are targeted at estrogen-ER signals[7–9]; in particular, selective ER modulators, including tamoxifen, are important therapies that increase the survival rate of patients[10–12]. Even though advancements have been made with respect to therapy, many women worldwide still die from breast cancer[13]. The serious problem that arises in patients is that during long-term endocrine therapy, the tumor often acquires drug resistance[14], and consequently it transforms into a more aggressive cancer[15,16].

Nuclear factor-κB (NF-κB) is a critical regulator of fundamental cell functions, including cell proliferation and survival[17,18]. This molecule usually exists as an inactive form in the cytoplasm by binding its endogenous inhibitor
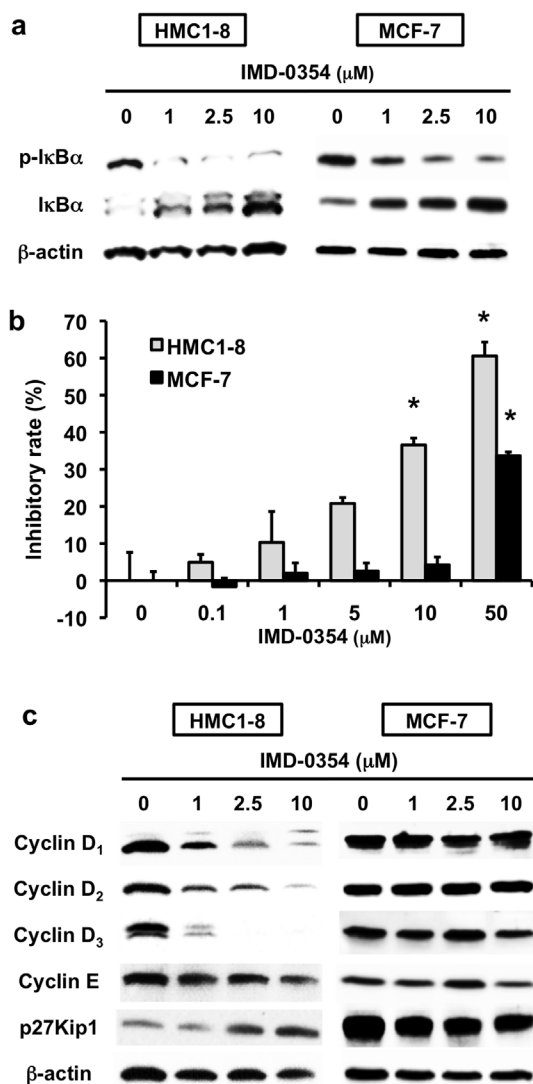
Figure 1 | NF-κB contribution to tumorigenic proliferation in ER-negative breast cancer cells. (a) Involvement of constitutive NF-κB activation in tumorigenic proliferation was examined using 2 different cell lines, namely, ER-positive MCF-7 and ER-negative HMC1-8 cells. After serum starvation, the cells were incubated in complete culture media with the indicated concentrations of IMD-0354 for 16 h; whole cell lysates were obtained to detect the IκB phosphorylation responsible for NF-κB activation by Western blot analysis. The constitutive phosphorylation of IκB and the downregulation of the phosphorylated form by IMD-0354 were detected in both cells. Concerning the expression of IκBα, 2 immunoreactive bands were identified in lysates from the HMC1-8 cells. The upper band was estimated as intact IκBα and the lower one was its partial proteolytic product. These cropped blots are used in the main figures and full-length blots are included in the supplementary information (Supplementary Fig. S1). Photos represent typical results obtained from 3 individual experiments. (b) The results obtained from the MTT assay revealed that NF-κB inhibition produced much stronger effects in HMC1-8 cells than in MCF-7 cells. Each column represents the mean ± SE of 4 different experiments in duplicates; *, $P < 0.01$ as compared with diluent controls. (c) The modulation of cell cycle regulatory proteins by NF-κB inhibition was analyzed by Western blot analysis. Cells were pre-incubated in serum-free media to decrease basal cell activation. Following overnight incubation, the cells were incubated for a further 24 h in complete media with increasing concentrations of IMD-0354, and the protein expressions of cell cycle regulatory proteins were detected. These cropped blots are used in the main figures and full-length blots are included in the supplementary information (Supplementary Fig. S3). Photos represent typical results obtained in 3 individual experiments.
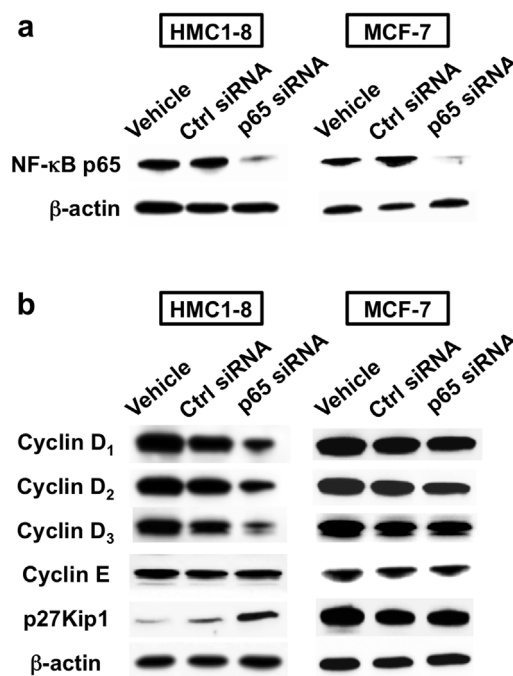

Figure 2 | Gene silencing by siRNA transfection against NF-κB p65 subunit. (a) ER-positive MCF-7 and ER-negative HMC1-8 cells were transfected with siRNA against the NF-κB p65 subunit (p65 siRNA) or control randomized sequences (Ctrl), and then the whole cell lysates were obtained. In both cells, siRNA successfully silenced the p65 gene. Vehicle alone was used as an untreated control (Vehicle). Photos represent typical results obtained in 3 individual experiments. These cropped blots are used in the main figures and full-length blots are included in the supplementary information (Supplementary Fig. S4). (b) In the HMC1-8 NF-κB-knockdown cells, D-type cyclins were suppressed and p27Kip1 levels were increased. The profile was similar to that in cells treated with IMD-0354. Comparatively, there was little change in their expressions in MCF-7 cells. Photos represent typical results obtained in 3 individual experiments. These cropped blots are used in the main figures and full-length blots are included in the supplementary information (Supplementary Fig. S5).

IκB. Following stimulation by bacterial lipopolysaccharide (LPS) or certain inflammatory cytokines[19], the phosphorylation of IκB is triggered by IκB kinases (IKKs), including subtype α and β. Phosphorylated IκB immediately undergoes proteolysis by the 26S proteasome and subsequently translocates to the nucleus[20], where NF-κB accelerates the transcription of target genes[18,19]. Importantly, abnormalities in this cascade have been reported in several malignancies, which suggests that NF-κB plays a key role in tumorigenesis[21–24]. Indeed, we have already demonstrated that NF-κB is crucial for tumorigenic proliferation of human breast cancer cells[24]. However, contribution of NF-κB to the malignant transformation of ER-positive breast cancers is poorly understood[25].

In most of the fatal cancers, including breast cancer, metastatic cancer cells systemically disseminate from the primary lesion, colonize distant organs, and extend metastatic lesions, which results in poor outcomes. In the process of metastasis, cancer cells must override numerous immunological, physiological, and mechanical barriers. In particular, the basement membrane is one of the most important obstacles during cell detachment from the primary site. Matrix metalloproteinases (MMPs) belong to a family of zinc-dependent endopeptidases and play an essential role in tissue homeostasis and tumor progression[26–29]. Among them, MMP-2 and MMP-9 are produced by invasive cancer cells because of their potent proteolytic abilities against the basement membrane[28]. MMP-9 is also produced by nonmalignant stromal cells such as fibroblasts or
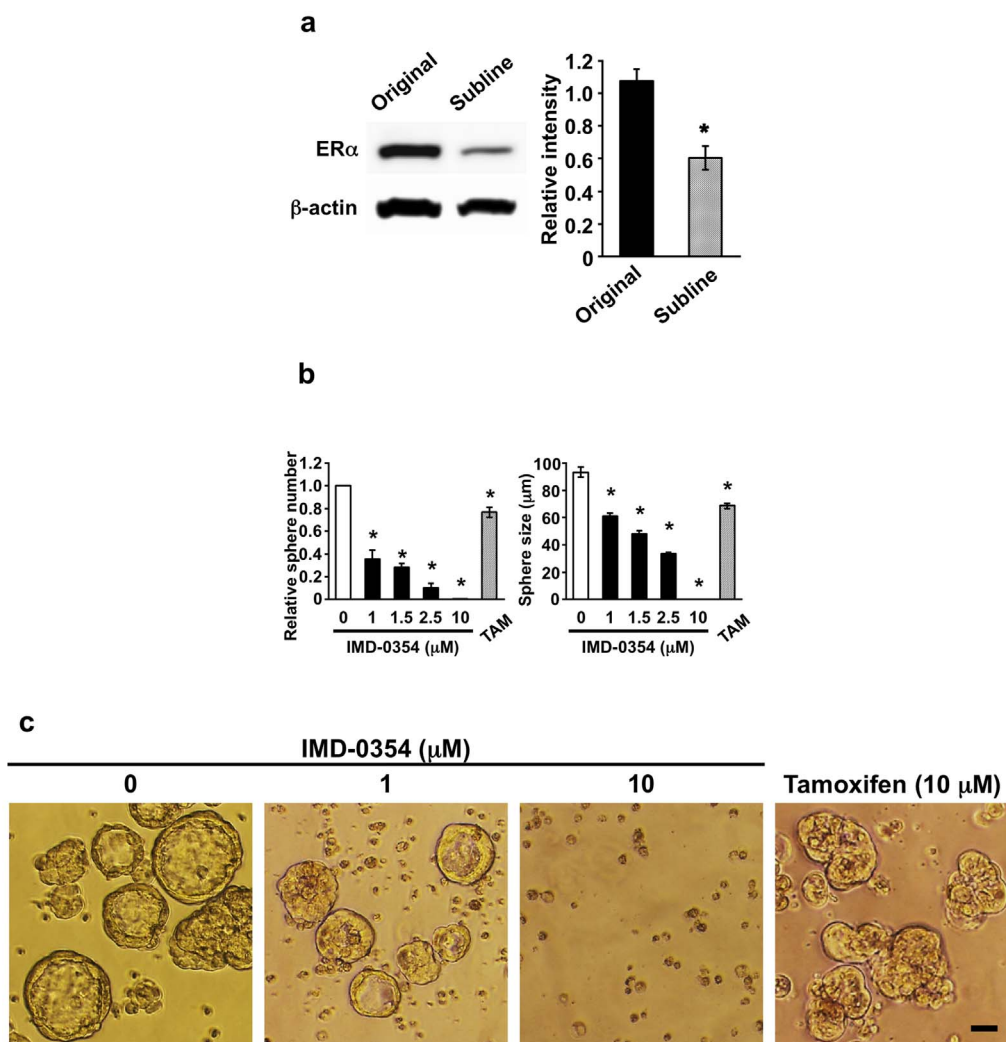
Figure 3 | Establishment of recurrent model with *de novo* resistance to endocrine therapy. To mimic the tumorigenesis of recurrent cancers in long-term endocrine therapy, a hormone-independent subline was obtained from original MCF-7 cells by incubation under estrogen-free conditions. (a) The subline exhibited not only hormone-independent growth in serum-deprived medium but also downregulation of ERα expression compared with the original cells. Photo represents the typical result obtained from 3 different examinations. Each column represents the mean ± SE of 3 different experiments in duplicates; *, $P < 0.01$ as compared with the original. These cropped blots are used in the main figures and full-length blots are included in the supplementary information (Supplementary Fig. S7). (b) Furthermore, they displayed low-responsiveness to tamoxifen (TAM). IMD-0354 (IMD) was more potently suppressive to proliferation of the subline when compared with the original (Fig. 1b and ref. 24). The number of spheres was calculated in triplicate per group and the relative sphere number was described as the ratio of treated value to control value. The sphere size was evaluated by measuring the maximum diameters of at least 50 spheres in each group. Each column represents the mean ± SE of 3 individual experiments; *, $P < 0.01$ as compared with the diluent control. (c) Photos demonstrate the representative features of cell morphology in each group from 3 individual experiments. Bars in photos indicate 20 μm.

infiltrating inflammatory cells, and their MMP-9 secretion is provoked by growth factors or inflammatory cytokines associating with cancer development[30]. Therefore, suppression of MMPs is another strategy for cancer therapy to interrupt invasion and metastasis.

In the present study, we developed an ER-reduced and tamoxifen-resistant subline that originated from ER-positive MCF-7 cells and focused on the roles of NF-κB in the transformed cells. Consistent with our previous findings, the proliferation of ER-negative breast cancer cells increased its dependency on NF-κB cascades. Furthermore, NF-κB inhibition enhanced ER expression and recovered tamoxifen sensitivity in the ER-reduced MCF-7 subline. This is the first report to demonstrate that altered dependency on the estrogen-ER axis may modify NF-κB sensitivity in breast cancer cells. Our findings also indicated that constitutive activation of NF-κB contributed to another malignant feature, namely, MMP-9-dependent invasive behavior; accordingly, this molecule may provide a potent therapeutic target for ER-positive and ER-negative breast cancers, including breast cancers that are weakly responsive to the conventional treatment.

Results

Abnormal activation of NF-κB both in ER-positive and ER-negative breast cancer cells. In order to examine the action of IMD-0354, which is a specific inhibitor targeted to IKKβ[31], we detected IκB phosphorylation in ER-positive MCF-7 and ER-negative HMC1-8 cells by Western blot analysis. As shown in Fig. 1a, constitutive phosphorylation of IκB leading to NF-κB activation was detected in both cell lines, and treatment with the IKKβ inhibitor successfully blocked their signals in a dose-dependent manner, regardless of ER expression. These photos of cropped blots represent typical results obtained from 3 individual experiments and full-length blots are included in Supplementary Fig.

S1. Concerning the immunobotting of HMC1-8 cell lysates, the IκBα antibody detected 2 immunoreactive bands approximately 30 kDa; however, the upper band was intact IκBα (predicted molecular weight: 36 kDa) and the lower band was considered its partial cleavage products of IκBα (Fig. 1a and Supplementary Fig. S1)[32]. DNA synthesis of ER-negative HMC1-8 cells was significantly suppressed by the addition of IMD-0354 even after 4 h (Supplementary Fig. S2). Interestingly, the suppressive effects of the IKKβ inhibitor on cell activities in the ER-positive cells were remarkably weaker than that in the ER-negative cells (Fig. 1b). Then, we compared the molecular mechanisms underlying enhanced cell cycle transition between ER-positive and ER-negative cells. Fig. 1c demonstrated spontaneous expression of cyclin D_1, D_2, D_3, and E in both lines. In the HMC1-8 cells, which lacked ER, treatment with IMD-0354 dramatically suppressed the expression of cyclin D_1, D_2, and D_3. Comparatively, IMD-0354 had little effect on the expression levels of the cyclins in the MCF-7 cells. The expression levels of cyclin E were not affected by NF-κB inhibition in both lines. Because the activities of the D-type cyclins are controlled by endogenous inhibitory molecules of cyclin-dependent kinase (CDK), which is a Cip/Kip family protein, we also analyzed whether IMD-0354 modulated the expression of p21Cip1/WAF1 and p27Kip1. The levels of p27Kip1 were increased in ER-negative cells, whereas there was no change in ER-positive cells. Regarding p21Cip1/WAF1, IKKβ inhibition produced no change in the expression levels with or without ER (data not shown). These cropped blots represent typical results obtained from 3 individual experiments and full-length blots are included in Supplementary Fig. S3.

Modulation of cell cycle regulatory proteins by NF-κB gene silencing. To confirm the effects of pharmacological inhibition, we silenced NF-κB gene expression by transfection with siRNA against the p65 subunit, which is one of the 2 subunits of NF-κB (p65 and p50). As shown in Fig. 2a, p65 siRNA successfully knocked down the gene in both cell lines analyzed. Predictably, NF-κB gene silencing induced suppression of D-type cyclins simultaneously with upregulation of p27Kip1 in HMC1-8 cells. In contrast, but similar to the results from the pharmacological IKKβ inhibition, there was little or no change detected in the MCF-7 cells. These data suggest that enhanced proliferation of ER-negative breast cancer cells may depend on NF-κB signaling, whereas ER-positive cells may grow in a NF-κB-independent manner in the presence of FBS that contains estrogen. These cropped blots describe typical results obtained from 3 individual experiments and full-length blots are presented in Supplementary Fig. S4 and S5.

Establishment of ER-reduced and tamoxifen-resistant subline as a recurrent breast cancer model. To analyze the resistant breast cancer phenotype to endocrine therapies, we established an in vitro recurrent model by incubating the cells under estrogen-free conditions (Supplementary Fig. S6). As shown in Fig. 3a, ERα was downregulated in the subline compared with the original cells, which resulted in the reduced estrogen dependency. These cropped blots describe typical results obtained from 3 individual experiments and full-length blots are presented in Supplementary Fig. S7. Tamoxifen is a competitive ER inhibitor and a preferred initial agent for endocrine therapy in ER-positive breast cancer; however, as shown in Fig. 3b and c, the inhibitory effects of tamoxifen on the hormone-independent subline were weaker. Therefore, the in vitro culture is available as an ER-positive but endocrine therapy-resistant breast cancer model for further investigation[14]. Comparatively, NF-κB inhibition dramatically suppressed cell growth compared with tamoxifen treatment. Furthermore, this subline showed a higher sensitivity to the blocking of NF-κB signals than the original cells. As already described in Fig. 1b, IMD-0354 had weaker inhibitory effect on proliferation of the original MCF-7 cells comparing to HMC1-8 cells. Similarly, we have already demonstrated, in our
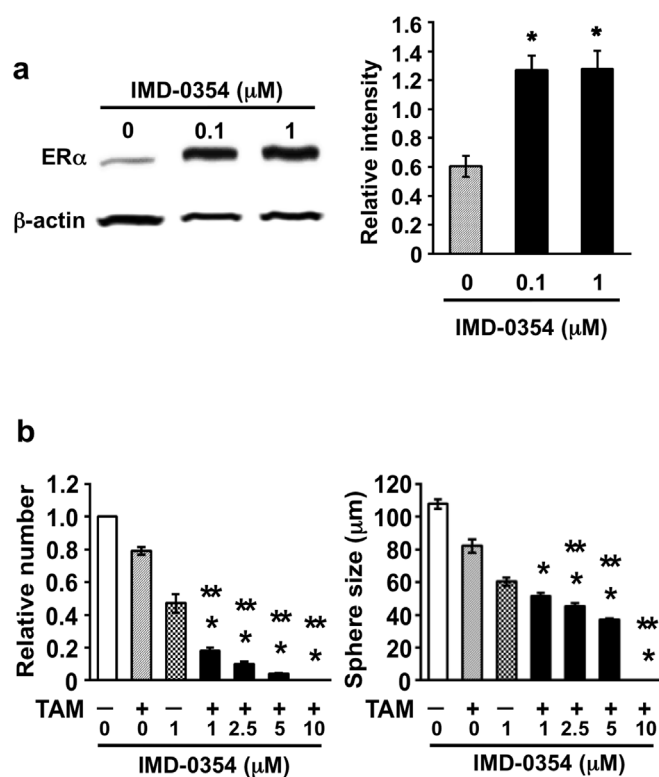

Figure 4 | Enhancement of tamoxifen sensitivity by NF-κB inhibition. (a) To determine the mechanisms of NF-κB-ER crosstalk, the expression levels of ERα were detected. The original MCF-7 cells were cultured in serum free and phenol red free AIM-V, and hormon-independent MCF-7 subline was obtained. Whole cell lysates were obtained from hormon-independent MCF-7 subline that was incubated in the indicated concentrations of IMD-0354 for 7 days, and then the ERα proteins were detected by Western blot analysis. These cropped blots represented data from 3 individual blots are used in the main figures and full-length blots are included in the supplementary information (Supplementary Fig. S8). Each value in the graph represents the mean ± SE of 3 different experiments; *, $P < 0.01$ as compared with diluent alone. (b) Concerning the therapeutic potential of NF-κB inhibition, the alternations to tamoxifen sensitivity were analyzed by combination treatment with IMD-0354. MCF-7 subline was incubated with tamoxifen (TAM, 10 μM) and increasing concentrations of IMD-0354 in estrogen-free media for further 7 days, and the number and diameter of the obtained spheres were measured using a microscope. Relative sphere numbers were normalized to the number in the medium alone. Each value represents the mean ± SE of 3 different experiments in triplicates; *, $P < 0.01$ as compared with tamoxifen alone, and **, $P < 0.01$ as compared with IMD-0354 alone.

previous report[24], that the original MCF-7 cells were resistant against IMD-0354 treatment. Taken together, our findings suggested that the subline strongly depends on NF-κB signaling for cell growth and survival.

NF-κB contribution to tamoxifen sensitivity through modulation of ERα expression. Contrary to the reduced estrogen dependency, the ER-reduced subline exhibited elevated NF-κB-dependent growth, which suggested crosstalk between the estrogen-ER axis and the NF-κB cascade. Therefore, we analyzed the interaction between ERα expression levels and NF-κB activities in the subline. Treatment with the NF-κB inhibitor induced ERα expression in a dose-dependent manner (Fig. 4a and full-length blots in Supplementary Fig. S8). Because the expression levels of ERα are a critical determinant of estrogen sensitivity and its depletion is a major cause of resistance against anti-estrogen chemotherapy, we
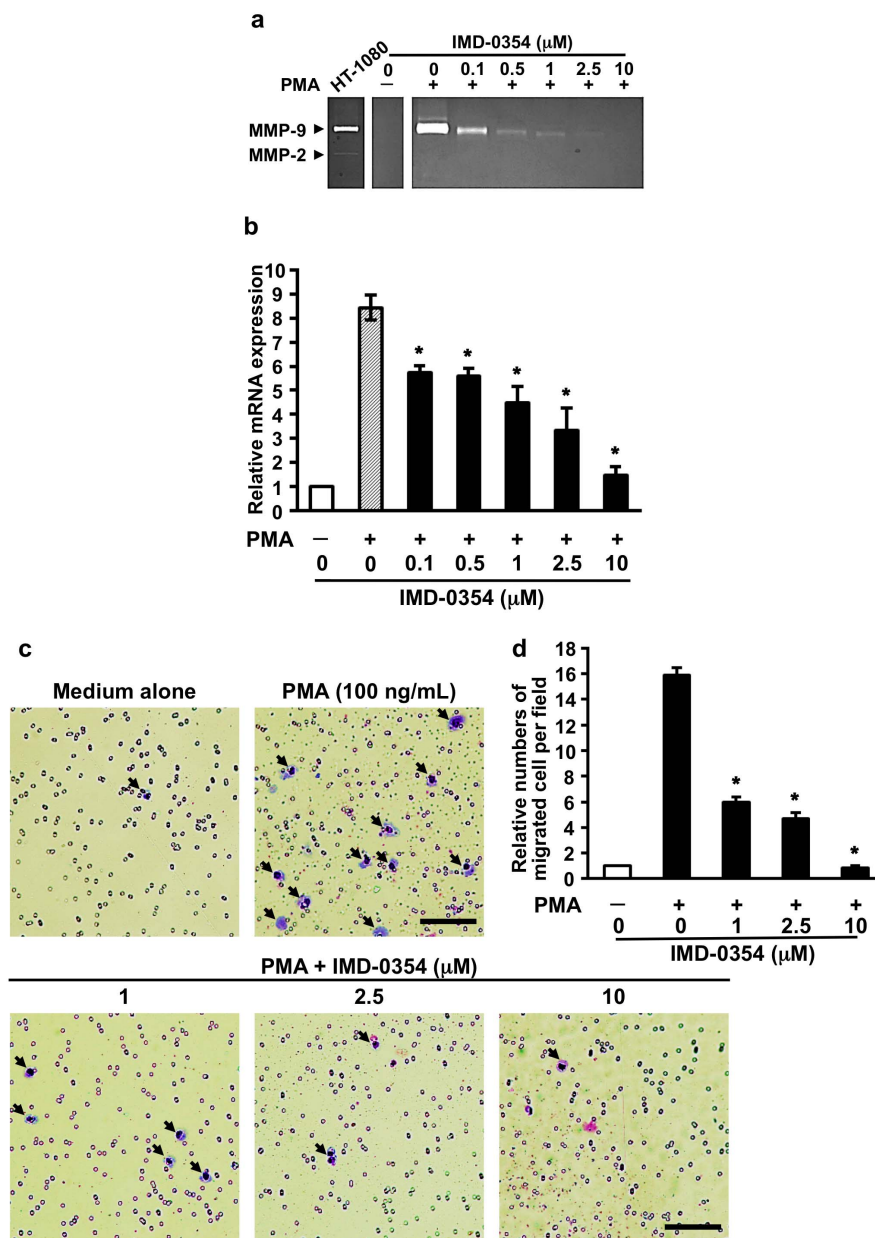
Figure 5 | Suppression of MMP-9-dependent invasive phenotype by NF-κB inhibition. To determine the NF-κB contribution to motility of cells, MMP-2/MMP-9 production was analyzed. (a) Original MCF-7 cells were incubated with the indicated concentrations of IMD-0354 in serum-free DMEM media for 48 h, and conditioned media were collected as samples for gelatin zymography. PMA (100 ng/mL) was used as a PKC activator. The 70-kDa and 90-kDa bands represent gelatinolytic activity of MMP-2 and MMP-9 in the conditioned media, respectively, and human fibrosarcoma HT-1080 cells were used as a positive control. These cropped gels are used in the main figures and full-length gels are included in the supplementary information (Supplementary Fig. S9). Photos are representative of 3 individual experiments. (b) PMA-induced MMP-9 activities were suppressed by IMD-0354. mRNA obtained from the MCF-7 cells was extracted at 16 h after the incubation begun, and then downregulation of *MMP-9* gene expression was detected by real-time RT-PCR. Each column represents the mean ± SE of 3 different experiments in duplicates; *, $P < 0.01$ as compared with PMA alone. (c) Furthermore, original MCF-7 cells were treated with various concentrations of IMD-0354 in the Matrigel-coated invasion chamber. After 24-h incubations, the cells invading into the Matrigel, which mimicked the basement membrane, were fixed, stained, and counted. Photographs show typical features of invading cells in each group. Arrows indicates migrated cells. Bars in photos indicate 200 μm. (d) Treatment of IMD-0354 for 24 h suppressed tumor cell invasion in a dose-dependent manner. Each value represents the mean ± SE of 3 different experiments in duplicates; *, $P < 0.01$ as compared with PMA alone.

evaluated the effects of NF-κB inhibition on tamoxifen sensitivity. As shown in Fig. 4b, treatment with tamoxifen and IMD-0354 showed synergistic effects on the inhibition of cell growth compared with tamoxifen alone. These photos of cropped blots show typical results obtained from 3 individual experiments and full-length blots are presented in Supplementary Fig. S8. The relative sphere number was normalized to control value and the sphere size was calculated

by measuring the maximum diameters of at least 50 spheres per group.

NF-κB involvement in acquisition of malignant phenotype. Because MMP-2 and MMP-9 degrade type IV collagen, which is a major component of basement membrane, these proteins are considered to be key molecules in distant metastasis development[28,33].
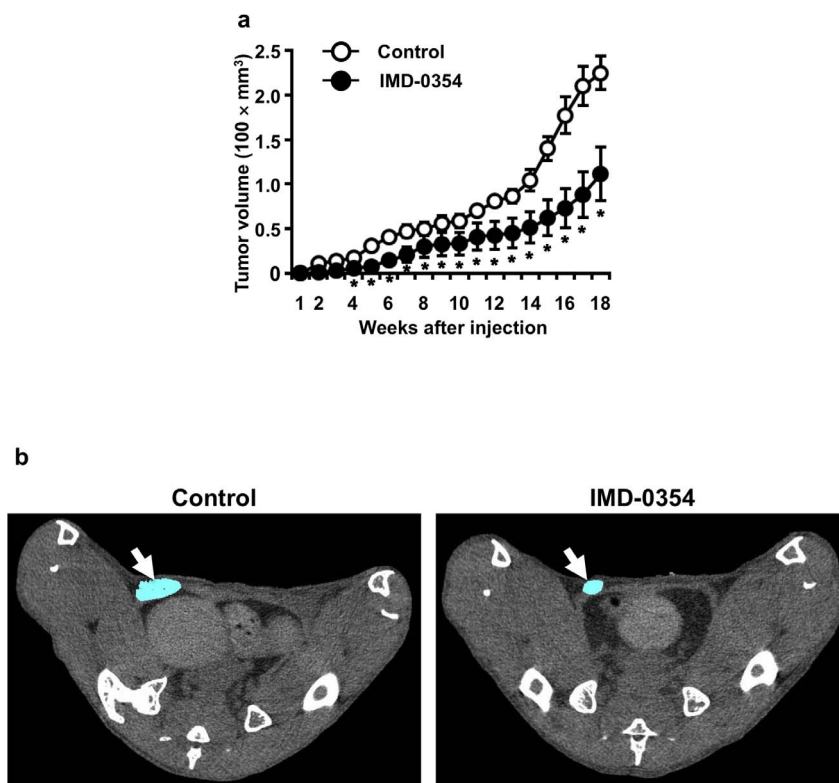
Figure 6 | Importance of NF-κB activation in breast cancer progression *in vivo*. To evaluate the contribution of NF-κB to tumor progression, *in vivo* studies were conducted. Original MCF-7 cells were pre-incubated with 2.5 μM of IMD-0354 to suppress cellular activities. Subsequently, the pre-treated cells were injected into mammary fat pads of female BALB/c-*nu/nu* mice (1×10^7 cells/100 μL PBS/mouse). (a) Tumor sizes were measured once a week, and pre-treatment with IMD-0354 suppressed tumor progression compared with the control PBS treatment. Each point indicates the mean ± SE of 2 different experiments with 7 mice in each group. (b) Computed tomography images of typical features of mice from each group. Areas indicated by white arrows show established tumors.

Fig. 5a demonstrates that while no gelatinolytic bands were detected in the conditioned media from the MCF-7 cells under steady-state conditions, the enzymatic activities corresponding to MMP-9 at approximately 90 kDa were dramatically induced by stimulation with PMA, and effectively suppressed by low-doses of IMD-0354. Comparatively, the basal levels of MMP-2, which is another potent gelatinase, were not detectable and PMA-stimulation failed to induce MMP-2 production. These clopped gels indicate the typical enzymatic activities obtained from 3 individual experiments and full-length gels are presented in Supplementary Fig. S9. RT-PCR analyses also clearly indicated that NF-κB inhibition also suppressed the PMA-induced *MMP-9* production in a dose-dependent manner (Fig. 5b).

Furthermore, to examine the effects on tumor cell behavior, we performed Matrigel migration assays, which evaluated the MMP-9-dependent cell migration *in vitro*. MCF-7 cells were incubated in serum-free DMEM media with increasing concentrations of IMD-0354 using Matrigel-coated transwell chambers; the numbers of the cells invading through the Matrigel, which mimicked the basement membrane, were counted. Twenty-four-hour incubation with IMD-0354 significantly suppressed the number of invasive cells stimulated by PMA in a dose-dependent manner (Fig. 5c and d). Photos demonstrate representative features of invading cells in each group.

NF-κB signals play an important role in tumor progression *in vivo*. Finally, to evaluate the pathogenic role of abnormal NF-κB activation, we performed *in vivo* studies using athymic nude mice. For suppression of cellular activity with a non-toxic dose of IMD-0354, MCF-7 cells were pre-treated with 2.5 μM of IMD-0354 in complete culture media for 24 h, and then injected into mouse mammary fat pads. Although NF-κB inhibition did not produce as

remarkable effects as the ER-negative cells, initial blockage of the cellular activities by IMD-0354 pre-treatment significantly suppressed tumor expansion in the nude mice implanted with MCF-7 tumors (Fig. 6a). In mice injected with the pre-treated cells, tumor progression was limited, as indicated in Fig. 6b.

Discussion

Constitutive phosphorylation of IκB was detected and blocked by IMD-0354 in ER-negative HMC1-8 and ER-positive MCF-7 cells. This suggests that abnormal activation of NF-κB is caused by IKKβ, which may be autoactivated or induced by ER-independent signals. However, the consequences of its activation vary depending on the presence of ER. In ER-negative cells, NF-κB is heavily involved in cell proliferation, mainly through the enhancement of D-type cyclins[21,34]. At the same time, activation of p27Kip1, which acts as a negative regulator through downregulation of the cyclin-D-CDK4 complex, was also elevated[35,36]. Expression levels of D-type cyclins determine entry into the DNA synthetic period, and their constitutive activation provokes enhanced cell proliferation and oncogenic transformation. Compared with ER-positive cells, which exhibit hormone-dependent growth, cell proliferation of ER-negative cells is predominantly dependent on the NF-κB-cyclin D axis instead of estrogen-ER pathways.

Because endocrine therapies have minimal success with ER-negative disease, the expression level of ERα is the most promising biomarker for both therapeutic strategies and prognosis predictions in breast cancers[37–39]. Our novel resistant model demonstrated that cell dependency on NF-κB was enhanced in the ER-reduced subline compared with the original cells, thereby suggesting that NF-κB signals play a central role in progression of resistant cancers, rather

than the estrogen-ER axis. Furthermore, ERα upregulation by IMD-0354 suggests that NF-κB activation induces downregulation of ERα, which is responsible for estrogen and tamoxifen sensitivities. Therefore, it is also possible that NF-κB inhibition restores the therapeutic efficacy of tamoxifen in recurrent cancers by induction of ERα expression[32,37–39].

Invasive and metastatic phenotypes are also prominent features of malignant cancers, and play a major role in clinical outcomes. PMA mimics pro-inflammatory conditions by activating protein kinase C, and the results from this study indicated that cells generate MMP-9, which enables basement membrane dissolution when they are stimulated by pro-inflammatory cytokines *in vivo*; furthermore, the results demonstrate that these phenomena critically depend on NF-κB signals. MMP-9 is mainly produced by nonmalignant stromal cells[30]. Therefore, the capacity of epithelial cancer cells to express MMP-9 is an important hallmark of malignant transformation that further highlights the importance of NF-κB in breast cancer tumorigenesis.

In conclusion, we focused on the inability to produce therapies to overcome breast cancers due to resistance to endocrine therapy. Our hypothesis was shown in Supplementary Fig. S10. Regarding ER-negative breast cancers, which demonstrate the most typical intrinsic resistance, there is strong evidence that abnormal NF-κB activation enhances cell cycle transition mainly by upregulation of D-type cyclins. Comparatively, in our recurrent model with *de novo* resistance (ER-reduced MCF-7), NF-κB signals played a critical role in cell growth and survival instead of the estrogen-ER cascade and enhanced the anticancer effects of conventional endocrine therapies on resistant cells. Furthermore, our results suggest that NF-κB contributes to tumor metastasis and progression and that NF-κB blockade may be an important key strategy to defeat human breast cancers.

Methods

Cell culture. Human breast cancer ER-positive MCF-7 and ER-negative HMC1-8 cells were provided by the Japan Health Science Foundation (Osaka, Japan), and MCF-7 cells were cultured in phenol red containing Dulbecco's modified Eagle's medium (DMEM; Life technologies, Carlsbad, CA) supplemented with 1% non-essential amino acids (Life technologies), 10% fetal bovine serum (FBS; Thermo Fisher Scientific Inc., Waltham, MA) and antibiotics. The estrogen (measured as estrone) concentration in FBS used in this study was 26 pg/ml. HMC1-8 cells were maintained in RPMI1640 (Life technologies) supplemented with 10% FBS and antibiotics.

Reagents. Rabbit anti-human phospho-IκBα antibody, rabbit anti-human β-actin antibody, and horseradish peroxidase (HRP)-conjugated secondary antibodies were obtained from Cell signaling Technology (Beverly, MA). Rabbit anti-human NF-κB p65 antibody, rabbit anti-human p27Kip1 antibody, rabbit anti-human cyclin D_1, rabbit anti-human cyclin D_2, rabbit anti-human cyclin D_3 antibody, rabbit anti-human cyclin E antibody, and rabbit anti-human ERα antibody were purchased from Santa Cruz Biotechnology (Santa Cruz, CA). The synthetic IKKβ inhibitor IMD-0354 (molecular weight, 384.1) was synthesized and kindly provided by the Institute of Medical Molecular Design Inc. (Tokyo, Japan)[31]. Unless otherwise indicated, all chemicals used in this study were obtained from Sigma-Aldrich (St. Louis, MO).

3-(4,5-Dimethylthiazol-2-yl)-2,5-diphenylterazolium bromide (MTT) assay. Both the MCF-7 and HMC1-8 cells (2×10^5 cells/mL) were incubated in phenol red-free media containing 10% FBS and antibiotics with various concentrations of IMD-0354. One hundred microliters of the cell suspension was applied to each well of the 96-well culture plates and incubated for 48 h. Four hours prior to the end of the culture period, 10 μL of 5 mg/mL MTT dissolved in phosphate-buffer saline (PBS) was added to each well. The reaction was stopped by adding 100 μL of 10% sodium dodecyl sulfate (SDS) in 0.01 N HCl. The absorbance was measured at 577 nm using an ImmunoMini NJ-2300 plate reader (Nalge Nunc International K.K., Tokyo, Japan). The mean of optical density (OD) was calculated in duplicates per group and then inhibitory rate (%) was evaluated according to the formula: Inhibitory rate (%) = {(control value − treated value)/control value} × 100.

Bromodeoxyuridine (BrdU) incorporation assay. The HMC1-8 cells (2×10^5 cells/mL) were incubated with elevated concentrations of IMD-0354. BrdU labeling was performed using a cell proliferation ELISA BrdU kit (Roche Applied Science, Penzberg, Germany) according to the manufacturer's instruction. Briefly, cells were treated with BrdU for 4 or 24 h at 37°C, washed in PBS, and fixed with fixative solution. After the cells were washed in PBS again, they were incubated with peroxidase-conjugated mouse anti-BrdU antibody for 60 min at 37°C. After

incubation in the substrate solution, the enzymatic reaction was stopped and the absorbance was measured at 450 nm using the ImmunoMini NJ-2300 plate reader (Nalge Nunc International K.K.). The mean of OD was calculated in duplicates per group and then inhibitory rate (%) was evaluated according to the formula: Inhibitory rate (%) = {(control value − treated value)/control value} × 100.

Western blot analysis. After the cells were washed in ice-cold PBS, 1×10^6 cells were lysed in 50 μL of CelLytic-M reagent (Sigma-Aldrich) supplemented with a protease inhibitor cocktail (Sigma-Aldrich). The supernatants were collected by centrifugation, mixed in equal amounts of 2 × sample buffer (20% glycerol, 10% 2-mercaptoethanol, 4% SDS, 100 mM Tris-HCl, and 0.01% bromophenol blue, pH 6.8), and boiled at 95°C for 7 min. The samples thus obtained were analyzed using SDS-polyacrylamide gel electrophoresis with 7.5% or 12.5% gels (Bio-Rad Laboratories, Hercules, CA), and separated proteins were transferred onto Immobilon-P membrane (Millipore, Bedford, MA). The membrane was blocked in 5% nonfat dry milk containing Tris-buffer saline (TBS) and blotted with primary antibodies diluted in a blocking solution. After washing in TBS containing 0.05% Tween-20, the membrane was incubated with HRP-conjugated secondary antibodies. Positive reactions were visualized using an Immobilon Western HRP substrate solution (Millipore).

Gene silencing by small interfering (si) RNA. After overnight incubation of the cells at a density of 1×10^5 cells/well in a 24-well culture plate, 50 nM siRNA against the NF-κB p65 subunit or control sequences (Cell Signaling Technology) was added to each well with the TransIT-TKO transfection reagent (Mirus Bio LLC, Madison, WI). After 48-h incubations, the samples for Western blot analysis were prepared from the transfected cells to determine their transfection efficiency as well as the expression levels of certain cell cycle regulatory proteins.

Establishment of hormone-independent subline. The hormone-independent MCF-7 subline was established under estrogen-free conditions. Original MCF-7 cells require estrogen contained in FBS for cell growth. Since phenol red in medium also exhibits estrogen-like activity[40,41], we incubated the cells in serum-free and phenol-red free AIM-V media (Life technologies) for 7 days, and obtained the estrogen-independent subline (Supplementary Fig. S6). Because those sublines exhibited a non-adherent phenotype and formed spheres (Supplementary Fig. 1S), for the evaluation of cell growth activities, original cells (1×10^5 cells/mL) were incubated with IMD-0354 or tamoxifen citrate (Millipore) in serum-free media for 7 days, and then the number and size of obtained spheres were measured. The mean of sphere number was found in triplicate in each group and the relative number was calculated according to the formula: Relative sphere number = treated value/control value. Concerning the sphere size, at least 50 spheres per group were randomly selected and the mean of maximum diameter was evaluated using the DP-21 microscope digital camera (Olympus Corporation, Tokyo, Japan).

Gelatin zymography assay. MCF-7 cells (2×10^5 cells/mL) were incubated in serum-free DMEM media with elevated concentrations of IMD-0354 in combination with 100 ng/mL of phorbol 12-myristate 13-acetate (PMA) for 48 h. After the cell debris was removed by centrifugation, the conditioned media were mixed in equal amounts of 2 × sample buffer (20% glycerol, 4% SDS, 125 mM Tris-HCl, and 0.01% bromophenol blue, pH 6.8). Next, the samples were electrophoresed in 10% SDS-polyacrylamide gel containing 0.1% gelatin (TEFCO, Tokyo, Japan) under non-reducing conditions. After electrophoresis, SDS was removed by incubation in 2.5% Triton X-100 for 30 min twice, and thereafter, the gels were incubated for 24 h at 37°C in 50 mM Tris-HCl buffer (pH 7.6) containing 1 mM $ZnCl_2$ and 5 mM $CaCl_2$. After fixation in 10% acetic acid/50% methanol, the gels were stained with 0.2% Coomassie Brilliant blue G-250 solution, and destained in a solution of 10% acetic acid/25% methanol. Gelatinolytic activities were detected by the appearance of negatively stained bands.

Real-time reverse transcription and polymerase chain reaction (RT-PCR) analysis. The total RNA was recovered from MCF-7 cells using a FastPure RNA kit (TAKARA BIO INC., Shiga, Japan) according to the manufacturer's instruction. The total RNA (2–5 μg) obtained from each sample was reverse-transcribed into cDNA using Oligo(dT)12–18 primers and the PrimeScript 1st strand cDNA Synthesis kit (Takara Bio Inc.). Reaction mixtures were amplified using a SYBR Premix Ex Taq II (Takara Bio Inc.) in the presence of 0.2 μmol/L of each of the sense and antisense primers for human MMP-9 (5′-CGTGTCTGGAGATTCCACTTGA-3′ and 5′-TGGAAGATGTCGTGTGAGTTCC-3′). The thermal cycling programs were stage 1, 95°C for 10 s; stage 2, 40 cycles of 95°C for 5 s and 60°C for 31 s; stage 3, 95°C for 15 s, 60°C for 1 min, and 95°C for 15 s. The fluorescence intensity was measured in real-time extension steps for a SYBR Green assay by using the ABI Prism 7000 Sequence Detector (PE Applied Biosystems, Tokyo, Japan). Glyceraldehyde-3-phosphate dehydrogenase (GAPDH) was used as an endogenous reference, and the relative expression levels of *MMP-9* gene were normalized by using the comparative CT (threshold cycle) method. The amount of gene expression that was normalized to the endogenous reference was given by $2^{-\Delta\Delta CT}$.

Invasion assay. For an invasion assay, BD BioCoat Matrigel Invasion chambers with a pore size of 8.0 μm were obtained from Becton, Dickinson and Company (Franklin Lakes, NJ). MCF-7 cells (2×10^5 cells/mL) were incubated in serum-free DMEM media with various concentrations of IMD-0354 in combination with 100 ng/mL

PMA. The cell suspensions (500 μL) were applied to the upper compartment of the invasion chamber, and 750 μL of culture media containing 10% FBS was added to the lower compartment. After incubation at 37°C for 24 h, the filter inserts were collected, fixed in 100% methanol, and stained using Diff-Quik stain (Sysmex Corporation, Hyogo, Japan). The cells that invaded through the Matrigel for chemotaxis to sera and localized to the underside of the filter were counted using a microscope (×200).

Tumor transplantation and *in vivo* experiments. MCF-7 cells pre-treated with 2.5 μM IMD-0354 for 24 h were suspended in PBS at a concentration of 1×10^8 cells/mL and subcutaneously injected into the mammary fat pad of 4–5-week-old female BALB/c nude mice (purchased from Charles River Japan, Inc., Yokohama, Japan; 1×10^7 cells/100 μL/mouse). As a control, the cells pre-incubated with PBS were injected into nude mice. All mice were maintained in an air-filtered specific pathogen-free condition, and tumor sizes were measured weekly. The estimated tumor volume was determined by the following formula: tumor volume (mm³) = [(width)² × length]/2. All experiments with animals complied with standards in the guidelines of the University Animal Care and Use Committee of the Tokyo University of Agriculture and Technology and were performed in accordance with the guidelines and regulation, which were approved by the institutional committee for experimental animals. The volume of tumors developed in the mammary fat pad was visualized by LaTheta® X-ray computed tomography (CT; Aloka, Tokyo, Japan) around the 5th lumbar vertebra, under inhalation anesthesia of isoflurane and were analyzed by visualization LaTheta® software according to the manufacture's instruction. Two individual experiments with 7 mice in groups were performed and computed tomography images of typical features of mice from both groups were visualized.

Statistical analysis. Comparison between multiple groups was analyzed by one-way analysis of variance (ANOVA), followed by a Tukey test as a post hoc test in *in vitro* experiments. In *in vivo* experiments, two-way ANOVA with a Tukey test was used. For the comparison between two groups, Student's t test was used. For all comparisons, a P value of < 0.01 was considered statistically significant.

1. Harvey, J. M., Clark, G. M., Osborne, C. K. & Allred, D. C. Estrogen receptor status by endocrine therapy in breast cancer. *J. Clin. Oncol.* **17**, 1474–1481 (1999).
2. Jensen, E. V. On the mechanism of estrogen action. *Perspect. Biol. Med.* **6**, 47–54 (1962).
3. Kuiper, G. G. *et al.* Cloning of a novel receptor expressed in rat prostate and ovary. *Proc. Natl. Acad. Sci. USA* **93**, 5925–5930 (1996).
4. Hamis, L. *et al.* American Society of Clinical Oncology 2007 update of recommendations for the use of tumor markers in breast cancer. *J. Clin. Oncol.* **25**, 5287–5312 (2007).
5. Hammond, M. E. *et al.* American Society of Clinical Oncology/College of American pathogenesis guideline recommendations for immunohistochemical testing of estrogen and progesterone receptors in breast cancer. *J. Clin. Oncol.* **28**, 2784–2795 (2010).
6. Wolff, A. C. *et al.* American Society of Clinical Oncology/College of American Pathologists guideline recommendations for human epidermal growth factor receptor 2 testing in breast cancer. *J. Clin. Oncol.* **25**, 118–145 (2007).
7. Cole, M. P., Jones, C. T. & Todd, I. D. A new anti-oestrogenic agent in late breast cancer. An early clinical appraisal of ICI 46474. *Br. J. Cancer* **25**, 270–275 (1971).
8. Fawell, S. E. *et al.* Inhibition of estrogen receptor-DNA binding by the "pure" anti-estrogen ICI 164,384 appears to be mediated by impaired receptor dimerization. *Proc. Natl. Acad. Sci. USA* **87**, 6883–6888 (1990).
9. Hoskins, J. M., Carey, L. A. & McLeod, H. L. CYP2D6 and tamoxifen: DNA matters in breast cancer. *Nature Rev. Cancer* **9**, 576–586 (2009).
10. Jensen, E. V. & Jordan, V. C. The estrogen receptor: a model for molecular medicine. *Clin. Cancer Res.* **9**, 1980–1989 (2003).
11. Riggs, B. L. & Hartmann, L. C. Selective estrogen-receptor modulators−Mechanisms of action and application to clinical practice. *N. Engl. J. Med.* **348**, 618–629 (2003).
12. Early Breast Cancer Trialists' Collaborative Group (EBCTCG). Effects of chemotherapy and hormonal therapy for early breast cancer on recurrence and 15-year survival: an overview of the randomized trials. *Lancet* **365**, 1687–1717 (2005).
13. Cancer Incidence, Mortality and Prevalence Worldwide in 2008, http://globocan.iarc.fr, International Agency for Research on Cancer, World Health Organization.
14. Musgrove, E. A. & Sutherland, R. L. Biological determinants of endocrine resistance in breast cancer. *Nature Rev. Cancer* **9**, 631–643 (2009).
15. Rhodes, L. V. *et al.* Cytokine receptor CXCR4 mediates estrogen-independent tumorigenesis, metastasis, and resistance to endocrine therapy in human breast cancer. *Cancer Res.* **71**, 603–613 (2011).
16. van Agthoven, T. *et al.* Relevance of breast cancer antiestrogen resistance genes in human breast cancer progression and tamoxifen resistance. *J. Clin. Oncol.* **27**, 542–549 (2009).
17. Oeckinghaus, A., Hayden, M. S. & Ghosh, S. Crosstalk in NF-κB signaling pathways. *Nature Immunol.* **12**, 695–708 (2011).
18. Pasparakis, M., Luedde, T. & Schmidt-Supprian, M. Dissection of the NF-κB signaling cascade in transgenic and knockout mice. *Cell Death Differ.* **13**, 861–872 (2006).
19. Hayden, M. S. & Ghosh, S. NF-κB in immunobiology. *Cell Res.* **21**, 223–244 (2011).
20. Scheidereit, C. IκB kinase complexes: gateways to NF-κB activation and transcription. *Oncogene* **25**, 6685–6705 (2006).
21. Perkins, N. D. The diverse and complex roles of NF-κB subunits in cancer. *Nat. Rev. Cancer* **12**, 121–132 (2012).
22. Frasor, J. *et al.* Positive cross-talk between estrogen receptor and NF-κB in breast cancer. *Cancer Res.* **69**, 8918–8925 (2009).
23. Zhou, Y. *et al.* Activation of nuclear factor-κB (NFκB) identifies a high-risk subset of hormone-dependent breast cancers. *Int. J. Biochem. Cell Biol.* **37**, 1130–1144 (2005).
24. Tanaka, A., Muto, S., Konno, M., Itai, A. & Matsuda, H. A new IκB kinase β inhibitor prevents human breast cancer progression through negative regulation of cell cycle transition. *Cancer Res.* **66**, 419–426 (2006).
25. Heldring, N. *et al.* Esrogen receptors: How do they signal and what are their targets. *Physiol. Rev.* **87**, 905–931 (2007).
26. Gross, J. & Lapiere, C. M. Collagenolytic activity in amphibian tissue: a tissue culture assay. *Proc. Natl. Acad. Sci. USA* **48**, 1014–1022 (1962).
27. Page-McCaw, A., Ewald, A. J. & Werb, Z. Matrix metalloproteinases and the regulation of tissue remodeling. *Nat. Rev. Mol. Cell Biol.* **8**, 221–233 (2007).
28. Kessenbrock, K., Plaks, V. & Werb, Z. Matrix metalloproteinases: regulators of the tumor microenvironment. *Cell* **141**, 52–67 (2010).
29. Egeblad, M. & Werb, Z. New functions for the matrix metalloproteinases in cancer progression. *Nat. Rev. Cancer* **2**, 161–174 (2002).
30. Sternlicht, M. D. & Werb, Z. How matrix metalloproteinases regulate cell behavior. *Annu. Rev. Cell Dev. Biol.* **17**, 463–516 (2001).
31. Tanaka, A. *et al.* A novel NF-κB inhibitor, IMD-0354, suppresses neoplastic proliferation of human mast cells with constitutively activated *c-kit* receptors. *Blood* **105**, 2324–2331 (2005).
32. Johnston, S. R. D. *et al.* Changes in estrogen receptor, progesterone receptor, and pS2 expression in tamoxifen-resistant human breast cancer. *Cancer Res.* **55**, 3331–3338 (1995).
33. Pan, Z. *et al.* Elevated expression of CUEDC2 protein confers endocrine resistance in breast cancer. *Nat. Med.* **17**, 708–714 (2011).
34. Berthois, Y., Katzenellenbogen, J. A. & Katzenellenbogen, B. S. Phenol red in tissue culture media is a weak estrogen: Implications concerning the study of estrogen-responsive cells in cuture. *Proc. Natl. Acad. Sci. USA* **83**, 2496–2500 (1986).
35. Devleeschouwer, N. *et al.* Growth factor-like activity of phenol red preparations in the MCF-7 breast cancer cell line. *Anticancer Res.* **12**, 789–794 (1992).
36. Chen, Z. *et al.* Signal-induced site-specific phosphorylation targets I kappa B alpha to the ubiquitin-proteasome pathway. *Genes Dev.* **9**, 1586–1597 (1995).
37. Padera, T. P. *et al.* Lymphatic metastasis in the absence of functional intratumor lymphatics. *Science* **296**, 1883–1886 (2002).
38. Barre, B. & Perkins, N. D. A cell cycle regulatory network controlling NF-κB subunit activity and function. *EMBO J.* **26**, 4841–4855 (2007).
39. Polyak, K. *et al.* p27Kip1, a cyclin-Cdk inhibitor, links transforming growth factor-β and contact inhibition to cell cycle arrest. *Genes Dev.* **8**, 9–22 (1994).
40. Xiong, X., Zhang, H. & Beach, D. Subunit rearrangement of the cyclin-dependent kinases is associated with cellular transformation. *Genes Dev.* **7**, 1572–1583 (1993).
41. Clarke, R. *et al.* Antiestrogen resistance in breast cancer and the role of estrogen receptor signalling. *Oncogene* **22**, 7316–7339 (2003).

Acknowledgements

Author contributions

K.O. performed experiments, analyzed data, wrote the paper, and prepared figures. A.M., K.J., Y.X. and H.J. supported the experiments and analyzed data. Y.A., G.A., S.N. and S.I. took care of animals used in the experiment and supported to prepare figures. E.J.J. and H.M. analyzed data and reviewed the manuscript. A.T. managed, directed, and financially supported all experiments and reviewed the manuscript. All authors reviewed the manuscript and agreed with the submission.

Additional information